Prognosis of Gestational Trophoblastic Neoplasia with Uterine Arteriovenous Malformation

Qing Zhou
Obstetrics & Gynecology Hospital of Fudan University
Yuantao Liu
Obstetrics & Gynecology Hospital of Fudan University
Xin Lu
Obstetrics & Gynecology Hospital of Fudan University
He Zhang
Obstetrics & Gynecology Hospital of Fudan University
Fenghua Ma
Obstetrics & Gynecology Hospital of Fudan University
Guofu Zhang (guofuzh@fudan.edu.cn)
Obstetrics and Gynecology Hospital of Fudan University https://orcid.org/0000-0001-9329-7314

Research Article

Keywords: gestational trophoblastic neoplasia, uterine arteriovenous malformation, placental site trophoblastic tumor, magnetic resonance imaging, contrast-enhanced magnetic resonance angiography

Posted Date: April 6th, 2022

DOI: https://doi.org/10.21203/rs.3.rs-1516122/v1

Abstract

Objective: This study investigated the prognosis of gestational trophoblastic neoplasia (GTN) with uterine arteriovenous malformation (UAVM) using contrast-enhanced magnetic resonance angiography(CE-MRA) as well as the correlation between UAVM and the prognosis for GTN to determine how to treat these diseases more effectively.

Methods: Forty-four patients with GTN at Obstetrics & Gynecology Hospital of Fudan University from December 2015 to December 2020 were selected. Imaging characteristics of conventional magnetic resonance imaging and contrast-enhanced magnetic resonance angiography (CE-MRA) before treatment, treatment methods, and the prognosis were followed-up.

Results: A total of 44 cases were included, including five cases of placental site trophoblastic tumor (PSTT) and 39 cases of GTN. There were two cases of PSTT combined with UAVM and 23 cases of GTN combined with UAVM. Thirty-nine cases of GTN were divided into two groups according to the presence or absence of UAVM. Data regarding the β-human chorionic gonadotropin value (<10,000 mIU/mL and ≥10,000 mIU/mL) were evaluated using Chi-square test ($P = 0.001$); the difference was statistically significant ($P < 0.05$). There was no significant difference in the International Federation of Gynecology and Obstetrics (FIGO) stage between groups ($P > 0.05$). The average FIGO scores of the two groups were 4.19 (±3.69) and 6. 70 (±3.39) ($P = 0.035$); the difference was statistically significant ($P < 0.05$).

Conclusion: The use of CE-MRA is helpful when diagnosing UVAM. The formation of UVAM is related to the prognosis score. The higher the prognosis score, the greater the possibility of UAVM.

Introduction

Gestational trophoblastic neoplasia (GTN) is a rare gynecological tumor that originates from placental trophoblastic cells and tends to occur in young women of childbearing age. GTN has strong vascular invasiveness and can be easily transferred to other parts of the body through blood circulation during the early stage, thus eroding the myometrium and forming local arteriovenous malformations (AVM). An AVM is the abnormal connection between arteries and veins of the capillary system. A uterine arteriovenous malformation(UAVM) is a part of the pathogenesis of GTN and results from uncontrolled proliferation of trophoblasts and invasion of the uterine myometrium. These vascular malformations are observed among 10–15% of patients, even after complete resolution of the tumor after chemotherapy. Overall, 1–2% of these uterine vascular malformations cause vaginal or intraperitoneal hemorrhage, which can be life-threatening [1]. This study aimed to gain a better understanding of the incidence of GTN complicated with UAVM and of the correlation between UAVM and the prognosis for GTN using contrast-enhanced magnetic resonance angiography (CE-MRA).

Materials And Methods

Patients

Data of 44 patients who were diagnosed with GTN at Obstetrics & Gynecology Hospital of Fudan University from December 2015 to December 2020 were collected. Before treatment, all patients underwent conventional magnetic resonance imaging (MRI) and CE-MRA examinations. The International Federation of Gynecology and Obstetrics (FIGO) 2000 clinical staging and prognosis scoring system was used to evaluate the severity of the condition and related risk factors, and the treatment methods (chemotherapy, surgical treatment, and arterial embolization) and prognosis determined during follow-up were recorded. Informed consent was signed by all patients before examination.

Inclusion criteria were an increased β-human chorionic gonadotropin (hCG) value after spontaneous abortion, ectopic pregnancy, or full-term pregnancy and metastases in the abdomen, lung, and brain, which are indicators of GTN. The components required to diagnose postmolar GTN include at least one of the following: β-hCG plateau over the course of 3 weeks or more; increase in β-hCG levels of 10% or more over the course of 2 weeks or more; β-hCG persistence 6 months or more after molar evacuation; histopathologic diagnosis of choriocarcinoma; and the presence of metastatic disease [2].

Exclusion criteria were pregnancy-related diseases, no evidence of GTN, previous arteriovenous malformations, and no available MRI or CE-MRA data.

Mri And Ce-mra Techniques

MRI was performed using a 1.5-T MRI system (Magnetom Avanto; Siemens, Erlangen, Germany) with a phased-array coil. During imaging, the patient was in the supine position and breathing calmly. The fast spin echo sequence was used for the MRI evaluation. T2-weighted imaging (T2WI) with fat suppression in the axial, sagittal, and coronal planes indicated a repetition time (TR) of 4000 ms and echo time (TE) of 83 ms. T1-weighted imaging (T1WI) with fat suppression in the axial plane indicated a TR of 761 ms, TE of 10 ms, field of view of 300 to 380 × 320 to 400 mm, matrix of 256 × 256 or 320 × 320, section thickness of 4.0 mm, and gap of 0.8 mm. The number of averages was 4.

CE-MRA images were acquired using real-time trigger technology. The scanning parameters were as follows: TR, 3.31 ms; TE, 1.2 ms; section thickness, 1.4 mm; gap, 0; number of averages, 1; and field of view, 400 to 450 mm. The scanning ranged from the upper edge of both kidneys to the symphysis pubis, and from the anterior edge of the external iliac artery to the posterior edge of kidney. The contrast media was 0.2 mmol/kg meglumine gadolinium pentanoate (Magnevist; Bayer Schering, Guangzhou Co., Ltd.). Rapid intravenous injection was performed manually, with an injection rate of approximately 2 mL/s. Thereafter, 20 mL of normal saline was injected. While injecting the contrast media, the care bolus sequence was used for real-time monitoring. When the contrast agent flowed through the external iliac artery, the first phase of the angiography sequence was manually triggered for scanning, scanning was performed for four consecutive phases, and the vascular images of the arterial phase and venous phase were obtained. After the fourth phase of scanning during the CE-MRA sequence, the conventional

enhanced sagittal and axial time spin echo T1WI sequence was performed, and the scanning parameters were the same as those of plain scanning.

The images were evaluated by two physicians with more than 10 years of experience with diagnostic MRI. The original images obtained by CE-MRA were reconstructed using two methods: maximum density projection and volume reconstruction. The supply artery and drainage vein of the lesion were observed from different angles. The maximum diameter of dilated blood vessels was measured at the widest part of the dilated vessels.

Statistical Analyses

Statistical analyses were performed using SPSS version 23.0. The normal distribution test was performed for the obtained data, and variables are expressed as means ± standard deviation (SD) and percentages. β-hCG values and FIGO stages of the two groups were compared using the chi-square test. The independent sample t-test was performed for the FIGO prognostic scores of the two groups. $P < 0.05$ was considered statistically significant.

Results

Statistics of general information

Among the 44 patients, 19 were treated surgically and five had a placental site trophoblastic tumor (PSTT) confirmed by pathology. Six cases were pathologically diagnosed as an invasive mole, three cases were diagnosed as choriocarcinoma, and five cases were clinically diagnosed as GTN. GTN cases excluding PSTT were evaluated together during this study. Patients were initially divided into two groups: the PSTT group and the GTN group. Two cases in the PSTT group were complicated with UAVM, and the maximum diameter of the dilated vessels was 8.95 (SD, ± 1.34 mm). Twenty-three cases in the GTN group were complicated with UAVM, and the maximum diameter of the dilated vessels was 13.79 mm (SD, ± 6.73 mm). In the PSTT group, five cases were treated with surgery; of these five cases, four were treated with adjuvant chemotherapy after surgery. These five cases were all cured. In the GTN group, 14 cases were treated with surgery, 6 cases were treated with multiple interventional therapy because of vaginal bleeding, and 39 cases were treated with adjuvant chemotherapy; of these cases, five were resistant and three relapsed. One patient was lost to follow-up. The mean β-hCG value of the PSTT group was 322.68 (SD, ± 549.41) mIU/mL; all values were < 10,000 mIU/mL (Table 1).

Table 1
Clinical characteristics

Variables	PSTT	Other GTN
n	5	39
Age, years	27.6 (± 1.52)	31.56 (± 9.79)
With UAVM	2	23
Maximum diameter of dilated vessels, mm	8.95 (± 1.34)	13.79 (± 6.73)
Surgery	5	14
Interventional therapy	0	6
Chemotherapy	4	39
CR	5	38
Drug resistance	0	5
Recurrent	0	3

CR, cured; GTN, gestational trophoblastic neoplasia; PSTT, placental site trophoblastic tumor; UAVM, uterine arteriovenous malformation.

Clinical Data Of The Gtn Group

The mean ages of the group without UAVM and the group with UAVM were 27.43 years (SD, ± 4.88) and 34.43 years (SD, ± 11.32), respectively ($P = 0.013$); this difference was statistically significant ($P < 0.05$). In the group without UAVM, regarding the last pregnancies, there were 12 GTN cases secondary to hydatidiform mole pregnancy, three GTN cases secondary to abortion, and one GTN case of unknown cause. In the group with UAVM, regarding the last pregnancies, there were 22 GTN cases secondary to hydatidiform mole pregnancy, two GTN cases secondary to abortion, and one GTN case secondary to full-term delivery; the pregnancy histories of two GTN cases were unknown. The data of those with β-hCG values < 10,000 mIU/mL and of those with β-hCG values ≥ 10,000 mIU/mL were tested by Chi-square test ($P = 0.001$); the difference was statistically significant ($P < 0.05$). The average FIGO prognostic scores of the two groups were 4.19 (SD, ± 3.69) and 6.70 (SD, ± 3.39) ($P = 0.035$ and $P < 0.05$). There was no significant difference in FIGO stages between the two groups ($P > 0.05$). In the group without UAVM, four cases underwent surgery, one case underwent interventional therapy, 11 cases underwent single-drug chemotherapy, five cases underwent combined chemotherapy, two cases developed drug resistance, and three cases relapsed. In the group with UAVM, 10 cases were treated with surgery, five cases were treated with interventional therapy, eight cases were treated with single-drug chemotherapy, 15 cases were treated with combined chemotherapy, three cases developed drug resistance, and no cases recurred (Table 2).

Table 2 Clinical characteristics of the two groups

Variables	Group A	Group B	*p*-value
	without UAVM	with UAVM	
N	16	23	
Age (years)	27.43 (± 4.88)	34.43 (± 11.32)	0.013
Last pregnancy			
Mole	12	18	
Abortion	3	2	
Term	0	1	
Unknown	1	2	
β-hCG value (mIU/mL)			0.001
< 10,000	12	5	
≥10,000	4	18	
Stage			0.365
I	6	5	
II	1	0	
III	8	17	
IV	1	1	
Prognostic risk score	4.19 (± 3.69)	6.70 (± 3.39)	0.035
0–6	11	11	
> 6	5	12	
Surgery	4	10	
Interventional therapy	1	6	
Chemotherapy regimen			0.037
Single-agent regimen	11	8	
Multiagent regimen	5	15	
Drug resistance	2	3	
Recurrent	3	0	

hCG, human chorionic gonadotropin; UAVM, uterine arteriovenous malformation.

Vascular Characteristics

In the PSTT group, there were two cases of an obvious tortuous dilated unilateral uterine artery, two cases of a dilated uterine vein with different degrees, one case of a dilated ovarian vein, and one case of an obvious dilated vaginal vein. In the GTN group, 23 cases were complicated with UAVM, a clear arterial image could not be obtained for one case, 12 cases had obvious unilateral uterine artery tortuosity and expansion, and 10 cases had obvious bilateral uterine artery tortuosity and expansion. Uterine veins were dilated in 22 cases. Nine cases were complicated with bilateral ovarian vein dilation. Eleven cases were complicated with unilateral ovarian vein dilation. One case had an obvious dilated vaginal vein (Table 3).

Table 3
Vascular characteristics

Group	Pelvic arteries			Pelvic veins		
	UA	OA	VA	UV	OV	VV
PSTT (n = 3)	3	0	1	3	1 (B)/1 (U)	1
Other GTN (n = 23)	22	1 (B)/1 (U)	1	22	9 (B)/11 (U)	1

UA, uterine artery; OA, ovarian artery; VA, vaginal artery; UV, uterine vein; OV, ovarian vein; VV, vaginal vein; B, bilateral; U, unilateral; PSTT, placental site trophoblastic tumor.

Discussion

According to the World Health Organization classification in 2020, GTN includes invasive hydatidiform mole, choriocarcinoma (hereafter referred to as choriocarcinoma), PSTT, and epithelioid trophoblastic tumor [3]. Invasive hydatidiform mole and choriocarcinoma comprise the majority of GTN cases. The principles of diagnosis and treatment of the two diseases are generally the same and involve referring to the FIGO stage and prognosis score [4, 5]. The two diseases were analyzed together as the GTN group during this study. PSTT and epithelioid trophoblastic tumor are rare but important forms of GTN with unique pathologies, natural histories, and treatment paradigms [6, 7]. They were analyzed together as the other GTN group during this study.

The statistics of this study suggest that the formation of UAVM is related to the prognosis score. The higher the prognosis score, the greater the possibility of UAVM.

Gestational trophoblastic tumors usually have a rich blood supply. Tumor cells have an erosive and reconstructive effect on blood vessels, forming masses that expand and distort vascular lesions. AVM is an abnormal connection between arteries and veins bypassing capillaries. UAVM is rare and can be caused by curettage, cesarean delivery, GTN, maternal diethylstilbestrol exposure, or endometrial and cervical tumors. The most common cause is GTN [8]. Studies have indicated that cesarean delivery

increases the risk of GTN after hydatidiform mole [9]. Another study [10] suggested that the formation of vascular lesions in the uterus is associated with placental tissue invasion in the myometrium and trauma. β-hCG may have a key regulatory role in angiogenesis and vascular function. High levels of β-hCG and unorganized trophoblast lead to destructive changes in the vascular structure and the likelihood of causing the arterial vessels to flow directly to venous vessels at the scar site to form UAVM [11]. The β-hCG value, as the first biomarker in the diagnosis, treatment, and follow-up of GTN, is high with an invasive hydatidiform mole and choriocarcinoma, but it is low with PSTT and epithelioid trophoblastic tumor [6]. During this study, the β-hCG value and prognosis score of the two groups were analyzed. The results suggested that when β-hCG was ≥ 10,000 mIU/mL, the probability of UAVM increased, and that the formation of UAVM is related to the prognosis score.

Two GTN cases with UAVM were also found in the PSTT group. The high β-hCG value may explain the cause of UAVM in these cases. However, β-hCG values were < 10,000 mIU/mL in the GTN group and PSTT group, and they may have been related to the complete angiogenesis between tumor cells in PSTT lesions and the infiltration of intermediate trophoblasts in the vessels. Touhami et al. [8] summarized 50 patients with GTN combined with UAVM in 14 works. The median hCG level at the time of AVM diagnosis was 2864.9 mIU/mL (range, 0–32,000), and three patients had undetectable hCG levels at the time of AVM diagnosis. During our study, β-hCG values during the early stage of treatment would have had greater reference value.

There were 25 cases of UAVM in this study; two of these UAVM cases included PSTT and 23 of these UAVM cases included GTN. The uterine arteries of all cases had different degrees of tortuous expansion, suggesting that the main blood supply of the focus came from the uterine artery. Ovarian artery imaging of two cases of GTN showed that the blood supply of the tumors was partly from the ovarian arteries. Uterine veins in all cases were dilated. Two cases of PSTT and 20 cases of GTN were complicated with unilateral or bilateral ovarian vein dilation, suggesting that the draining veins of the lesions were uterine veins and ovarian veins. Dilated ovarian veins may cause the formation of local UAVM, which leads to the expansion of the pelvic vein volume and an increase in the total pelvic vessel pressure along with the reflux mode of ovarian vein resistance and the lack of venous valve, resulting in the expansion of the ovarian vein and early observation of the arterial phase with CE-MRA [12].

Approximately 10–15% of patients experience GTN combined with UAVM. However, it appears that only 2% of uterine AVMs are symptomatic and cause chronic or heavy bleeding [1]. Some patients also experience pelvic pain. Some studies have shown that even after GTN is completely cured, UAVM still exists and poses the risk of massive hemorrhage. UAVM will cause bleeding and influence the effects of intravenous chemotherapy because the arterial blood carrying a large number of chemotherapy drugs does not enter the focus tissue and flows directly back into the vein, leading to ineffective circulation of chemotherapy drugs. During this study, drug resistance occurred in two cases in the group without UAVM and in three cases in the group with UAVM. Considering the small number of cases, whether UVAM will cause drug resistance requires follow-up research. The most effective treatment for UAVM complicated with massive hemorrhage is interventional therapy. The success rate of interventional therapy is 78.6–

90% [13–16]. Interventional therapy can control the bleeding caused by UAVM and treat the bleeding caused by the primary focus and metastasis. During this study, six patients underwent interventional embolization because of vaginal bleeding; of these patients, five had UAVM. All six patients underwent CE-MRA before interventional therapy, and hemorrhage was effectively controlled in every patient.

The gold standard for the diagnosis of UAVM is interventional angiography. However, this technique is invasive and exposes the patient to a certain amount of ionizing radiation. MRI has advantages in the diagnosis of GTN combined with UAVM [14, 17, 18]; for example, it can obtain the vascular characteristics of the feeding arteries and drainage veins, provide a reference for the design of the interventional treatment scheme, shorten the interventional time, and reduce the radiation dose experienced by physicians and patients during interventional surgery. The time-resolved CE-MRA sequence can be used to observe UAVM combined with ovarian venous dilatation reflux and the whole process of blood circulation, to clarify the circulation characteristics of the tumor vessels, and to provide a reference for subsequent treatment [19].

The formation of UVAM is related to the prognosis score. The higher the prognosis score, the greater the possibility of UVAM. CE-MRA is helpful for diagnosing UVAM in a timely manner, thereby preventing life-threatening massive bleeding and providing a better reference for follow-up treatment.

Figures

Declarations

Author contribution

Qing Zhou: Project development, Data collection, Manuscript writing

Yuan-tao Liu: Data collection, Data analysis, Manuscript writing

Xin Lu: Supervision, Revising

He Zhang: Revising

Feng-hua Ma: Project development, Data collection, Revising

Guo-fu Zhang: Project development , Supervision, Revising

References

1. Lim AK, Agarwal R, Seckl MJ, Newlands ES, Barrett NK, Mitchell AW (2002) Embolization of bleeding residual uterine vascular malformations in patients with treated gestational trophoblastic tumors. Radiology 222(3):640–644. doi: 10.1148/radiol.2223010035

2. Lurain JR (2011) Gestational trophoblastic disease II: classification and management of gestational trophoblastic neoplasia. Am J Obstet Gynecol 204(1):11–18. doi:10.1016/j.ajog.2010.06.072
3. Seckl MJ, Sebire NJ, Berkowitz RS (2010) Gestational trophoblastic disease. Lancet 376(9742):717–729. doi:10.1016/S0140-6736(10)60280-2
4. Ngan HYS, Seckl MJ, Berkowitz RS, Xiang Y, Golfier F, Sekharan PK et al (2018 Oct) Update on the diagnosis and management of gestational trophoblastic disease. Int J Gynaecol Obstet 143(Suppl 2):79–85. doi:10.1002/ijgo.12615
5. Silva ALMD, Monteiro KDN, Sun SY, Borbely AU (2021 Dec) Gestational trophoblastic neoplasia: Novelties and challenges. Placenta 116:38–42. doi: 10.1016/j.placenta.2021.02.013
6. Hyman DM, Bakios L, Gualtiere G, Carr C, Grisham RN, Makker V et al (2013 Apr) Placental site trophoblastic tumor: analysis of presentation, treatment, and outcome. Gynecol Oncol 129(1):58–62. doi:10.1016/j.ygyno.2012.12.029
7. Gadducci A, Carinelli S, Guerrieri ME, Aletti GD (2019) Placental site trophoblastic tumor and epithelioid trophoblastic tumor: Clinical and pathological features, prognostic variables and treatment strategy. Gynecol Oncol 153(3):684–693. doi:10.1016/j.ygyno.2019.03.011
8. Giurazza F, Corvino F, Silvestre M, Cavaglià E, Amodio F, Cangiano G et al (2021 Feb) Uterine Arteriovenous Malformations. Semin Ultrasound CT MR. 42:37–45. 10.1053/j.sult.2020.08.00. 1
9. Cho HW, Ouh YT, Min KJ, Lee NW, Lee S, Song JY et al (2020 Mar) The impact of previous cesarean section (C/S) on the risk for post-molar gestational trophoblastic neoplasia (GTN). Gynecol Oncol 156(3):606–610. doi:10.1016/j.ygyno.2019.11.032
10. Ju da H, Yi SW, Sohn WS, Lee SS (2015) Acquired uterine vascular abnormalities associated with persistent human chorionic gonadotropin: Experience at a Korean teaching hospital. Taiwan J Obstet Gynecol 54(6):654–659. doi:10.1016/j.tjog.2014.06.008
11. Touhami O, Gregoire J, Noel P, Trinh XB, Plante M (2014) Uterine arteriovenous malformations following gestational trophoblastic neoplasia: a systematic review. Eur J Obstet Gynecol Reprod Biol 181:54–59. doi:10.1016/j.ejogrb.2014.07.023
12. Asciutto G, Asciutto KC, Mumme A, Geier B (2009) Pelvic venous incompetence: reflux patterns and treatment results. Eur J Vasc Endovasc Surg 38(3):381–386. doi:10.1016/j.ejvs.2009.05.023
13. Molvi SN, Dash K, Rastogi H, Khanna SB (2011) Transcatheter embolization of uterine arteriovenous malformation: report of 2 cases and review of literature. J Minim Invasive Gynecol 18(6):812–819. doi:10.1016/j.jmig.2011.07.007
14. Lim AK, Agarwal R, Seckl MJ, Newlands ES, Barrett NK, Mitchell AW (2002 Mar) Embolization of bleeding residual uterine vascular malformations in patients with treated gestational trophoblastic tumors. Radiology 222(3):640–644. doi:10.1148/radiol.2223010035
15. Kim T, Shin JH, Kim J, Yoon HK, Ko GY, Gwon DI et al Management of bleeding uterine arteriovenous malformation with bilateral uterine artery embolization.Yonsei Med J. 2014Mar; 55(2):367–73. doi: 10.3349/ymj.2014.55.2.367

16. Cura M, Martinez N, Cura A, Dalsaso TJ, Elmerhi F (2009) Arteriovenous malformations of the uterus. Acta Radiol 50(7):823–829. doi:10.1080/02841850903008792
17. Szpera-Goździewicz A, Gruca-Stryjak K, Bręborowicz GH, Ropacka-Lesiak M (2018) Uterine arteriovenous malformation - diagnosis and management. Ginekol Pol 89(5):276–279. doi:10.5603/GP.a2018.0047
18. Shaaban AM, Rezvani M, Haroun RR, Kennedy AM, Elsayes KM, Olpin JD et al Gestational Trophoblastic Disease: Clinical and Imaging Features.Radiographics. 2017 Mar-Apr; 37(2):681–700. doi: 10.1148/rg.2017160140
19. Kim CY, Miller MJ Jr, Merkle EM (2009) Time-resolved MR angiography as a useful sequence for assessment of ovarian vein reflux. AJR Am J Roentgenol 193(5):W458–W463. doi:10.2214/AJR.0

Figures

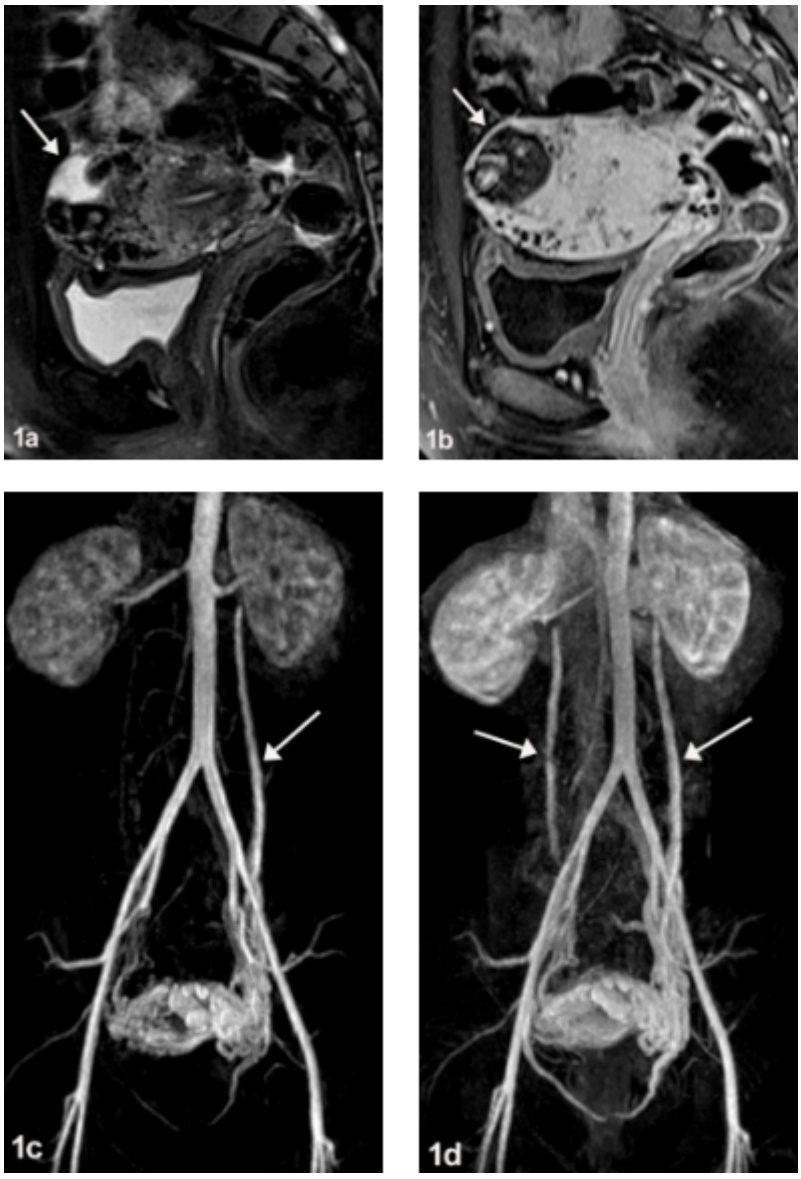

Figure 1

Invasive mole in a 24-year-old woman who had ascending human chorionic gonadotropin (hCG) levels after molar pregnancy. Sagittal T2-weighted imaging (T2WI) with fat suppression (FS) (a) shows a hyperintense mass (arrow) centered on the anterior myometrium. Multiple signal voids (enlarged vascular structures) are observed in the mass and adjacent myometrium. Sagittal contrast-enhanced T1-weighted imaging (T1WI) with FS (b) shows that the mass has heterogeneous enhancement (arrow). There are multiple tortuous blood vessels in the uterine area during the early arterial phase (c), and the left ovarian vein is seen (arrow). Both enlarged ovarian veins are shown during the late arterial phase (d).

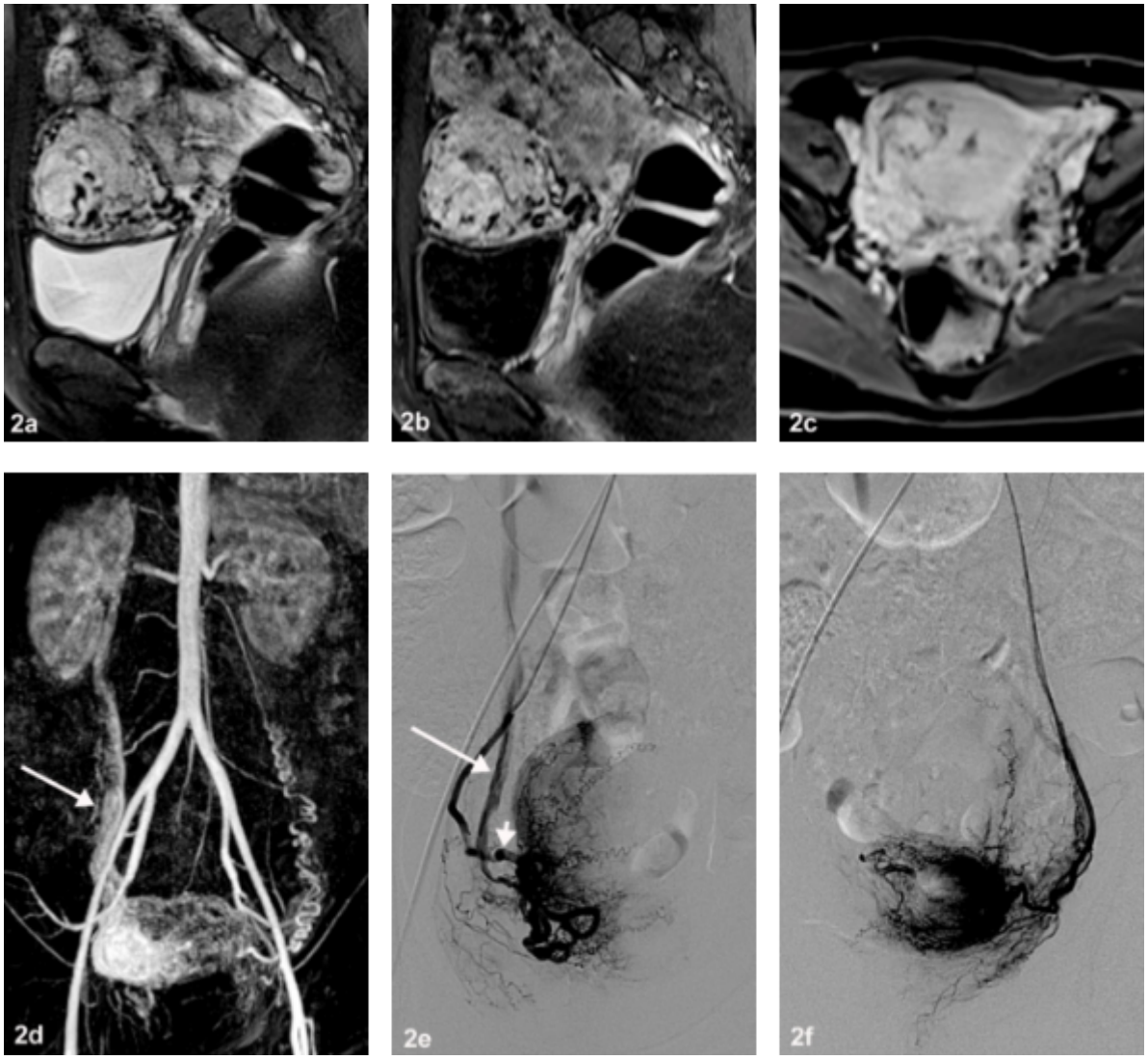

Figure 2

A 32-year-old woman with massive vaginal bleeding 2 weeks after the initiation of treatment for a gestational trophoblastic neoplasia (GTN) (III: 4). (a-d) Before chemotherapy. Sagittal T2-weighted imaging (T2WI) shows (a-c) a hyperintense mass (arrow) in the right myometrium. Contrast-enhanced magnetic resonance angiography (CE-MRA) (d) shows tortuous blood vessels on both sides of the uterus. The ovarian veins of both sides are tortuous and thickened. Two months after chemotherapy, the patient was admitted to the hospital for heavy vaginal bleeding. (e and f) Images of uterine artery embolization. Right internal iliac artery angiogram (e) during the arterial phase shows opacification of an enlarged right

uterine artery (short arrow) and a nidus of contrast material and blush (long arrow) with ovarian venous drainage. Left internal iliac artery angiogram (f) during the arterial phase shows opacification of an enlarged left uterine artery.

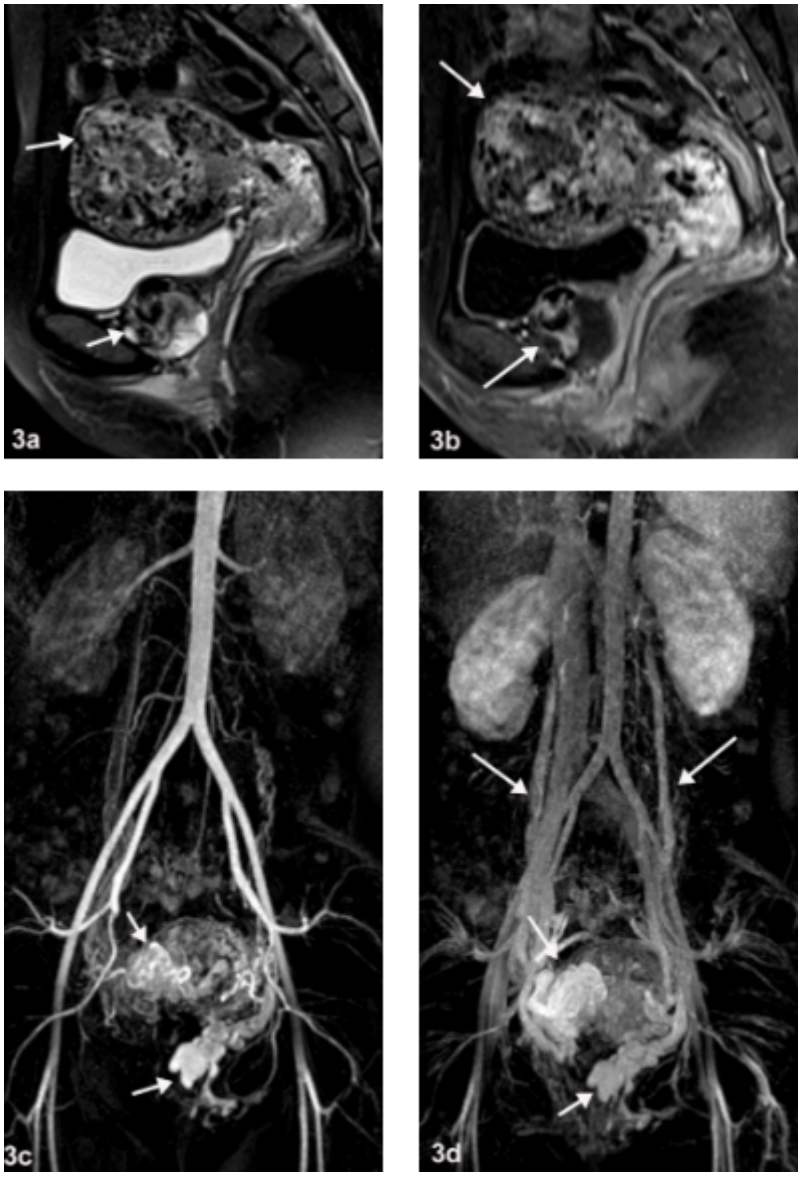

Figure 3

Placental site trophoblastic tumor (PSTT) in a 25-year-old woman with vaginal bleeding 6 months after full-term vaginal delivery. Sagittal T2-weighted imaging (T2WI) with fat suppression (FS) (a) shows a diffuse heterogeneous signal area in the myometrium with unclear boundaries. Sagittal contrast-enhanced T1-weighted imaging (T1WI) with FS (b) shows a mass with mixed signals on the anterior wall of the vagina (arrow). There are multiple tortuous blood vessels in both the uterine area and vaginal area during the early arterial phase (c). Both enlarged ovarian veins are shown during the late arterial phase (d).